KSCE Journal of Civil Engineering (2014) 18(1):182-187

DOI 10.1007/s12205-014-0056-7

Highway Engineering

pISSN 1226-7988, eISSN 1976-3808
www.springer.com/12205

Effect of Temperature-induced Load on Airport Concrete Pavement Behavior

Sung-Hee Kim*, Joo-Young Park, and Jin-Hoon Jeong*****

Received January 26, 2013/Accepted April 12, 2013

Abstract

In many countries, airport pavements are designed according to the Federal Aviation Administration (FAA) Rigid and Flexible Iterative Elastic Layer Design (FAARFIELD) program. FAARFIELD is capable of analyzing airport pavement behavior based on both the layered elastic-based and three-dimensional finite-element-based design methods. Although the FAA design methods accommodate the mechanical principles needed to calculate the slab thickness required for a given aircraft fleet mix, the effect of temperature-induced loading on the concrete pavement behavior is not considered. This paper presents the tensile stress distribution of concrete slabs and the landing gear position where the maximum tensile stress is observed when both load-induced and temperature-induced loads are taken into consideration in the analysis. Based on three-dimensional finite element analyses, it was observed that the distress types and locations coincided with the actual distress types and locations that are typically found in the field when both traffic-induced and temperature-induced loadings were considered in the analysis.

Keywords: *airport, concrete pavement, temperature, Coefficient of Thermal Expansion (CTE), Mechanistic-Empirical Pavement Design Guide (MEPDG)*

1. Introduction

Airport pavements are designed according to the Federal Aviation Administration (FAA) Rigid and Flexible Iterative Elastic Layer Design (FAARFIELD) program. Both layered elastic-based and three-dimensional finite-element-based design methods are implemented in FAARFIELD. For rigid pavement design, the maximum horizontal stress at the bottom edge of a Portland Cement Concrete (PCC) slab is calculated under an edge loading condition and is used as an indicator to obtain the pavement's structural life. The FAA design methods accommodate the mechanical principles needed to calculate the slab thickness required for a given aircraft fleet mix. Although FAARFIELD considers the traffic loadings in airport pavement design, the temperature loading is not taken into consideration.

It is well known that concrete expands as the temperature increases and contracts as the temperature decreases (Kim *et al.*, 2013). The Coefficient of Thermal Expansion (CTE) is a key parameter for highway pavement design because concrete mixtures with high CTEs are generally subjected to severe temperature-related pavement deteriorations such as spalling, faulting, and corner cracking. Significant efforts have been made to prevent these temperature-related pavement deteriorations by investigating the effect of the concrete mix design variables on CTE, so that the maximum CTE can be limited in rigid pavement design.

To consider CTE in an airport pavement analysis, the CTEs for prepared concrete mixtures were measured in accordance with AASHTO T336-11 (AASHTO, 2011). These measured CTEs were used as input values for the finite element program to estimate the tensile stress of a concrete slab in conjunction with traffic loading. By considering the effects of both the traffic-induced and temperature-induced loadings on a concrete slab, airport pavement deterioration can be properly understood and designed to minimize foreign object debris, which can damage aircraft and injure people when thrown into the air by a jet blast.

2. Nondestructive Testing of Test Section

A test section of an airport pavement in Kentucky, USA was selected, and pavement cores from the test section were extracted to identify the existing pavement thickness and composition. The pavement profile is tabulated in Table 1. Falling Weight Deflectometer (FWD) tests were conducted in the test section to obtain the field subgrade reaction (k). Most of these tests were conducted under an impulse (i.e., FWD) forcing function at a nominal amplitude of 111 kN (25 kips) at each test location. The

*Associate Professor, Dept. of Civil and Construction Engineering, Southern Polytechnic State University, Marietta, GA 30060, USA (E-mail: skim4@spsu.edu)
**Ph.D. Candidate, Dept. of Civil Engineering, Inha University, Incheon 402-751, Korea; Currently, Assistant Manager, Civil Engineering Center, Samsung C&T, Seoul 137-956, Korea (E-mail: jy0704.park@samsung.com)
***Member, Associate Professor, Dept. of Civil Engineering, Inha University, Incheon 402-751, Korea (Corresponding Author, E-mail: jhj@inha.ac.kr)

Table 1. Test Section Profile

	PCC	CTB	AGBS	Subbase
Thickness (mm)	432	152	305	610

*Note:
– PCC: Portland Cement Concrete
– CTB: Cement Treated Base
– AGBS: Aggregate Base

tests were generally conducted at intervals of approximately 15 m in the middle of the test section. The FWD used seven response-monitoring sensors to record data. These sensors were placed at the center of the loading plate and at radial offsets of 203, 457, 610, 914, 1219, and 1524 mm. To obtain a meaningful database for evaluating the test section, the following NDT sequences were used:

- Deflection Basin
- Impulse Stiffness Modulus

The NDT equipment, test procedures, and data reduction methods conformed to the requirements of FAA Advisory Circular 150/5370-11A (FAA, 2011), "Use of NDT Equipment in the Evaluation of Airport Pavements. The deflection basin test involves measuring the deflection at the center of the machine's loading plate and at fixed distances from the center. Based on the pavement thickness and composition listed in Table 1, closed-form back-calculation procedures and layered elastic back-calculation procedures were used to reduce the NDT data for the test section. Both the closed-form procedures and layered elastic back-calculation methods are also discussed in Advisory Circular 150/5370-11A (FAA, 2011). As described in the FAA Advisory Circular 150/5370-11A, layered elastic back-calculation procedures can be used to process deflection basin data to compute the set of elastic modulus (E) values that provides the best fit between the measured and computed deflection basin data. The closed-form procedures are based on computing the normalized area (AREA) under the deflection basin. As discussed in the FAA advisory circular, a unique relationship has been shown between AREA and the radius of the relative stiffness (l) of the concrete pavement. Once l is known, computing the modulus of the subgrade reaction (k) and the elastic modulus of the concrete slabs (E) is straightforward. Both k and E were computed for each NDT location.

The Impulsive Stiffness Modulus (ISM) is defined as the dynamic force divided by the pavement deflection at the loading plate. As such, it is a measure of the overall support conditions from all influencing pavement and subgrade layers. For this study, the ISM data were used to segment the pavement section into statistically equivalent areas for structural analysis and to identify the patterns of variability in the pavement support conditions. An examination of the NDT field data found some variability in the support conditions for the various pavement areas that were tested. Plots of ISM versus the location are shown in Fig. 1. From the ISM measurements, the elastic modulus and California Bearing Ratio (CBR) value were estimated and tabulated in Table 2. As shown in Table 2, the mean and standard deviation of the

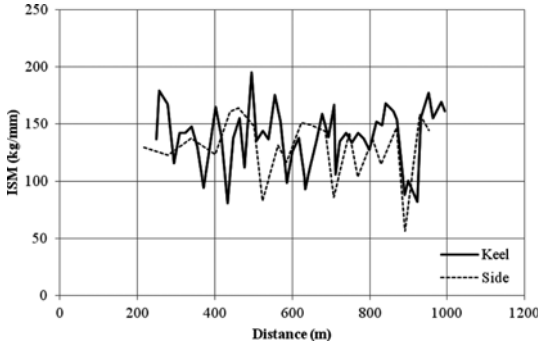

Fig. 1. ISM Plot of Test Section

Table 2. Back-Calculation Results

Design E (MPa)	Design CBR (%)	Design k (MPa/mm)	Avg. ISM (kg/mm)
158	15.3	0.03	138

Table 3. Aircraft Fleet Mix

Aircraft Type	Weight (kg)	Gear	Repetition
Narrow-Body Jets			
B727	78,018	D	1
B737-300	63,503	D	1
B737-400	68,266	D	0
B737-700	69,626	D	14
B737-800	78,471	D	2
B757	113,398	2D	11
A300	170,097	2D	23
A319, 320	73,482	D	1
DC9 Series	55,338	D	2
F100	45,813	D	1
MD80 Series	73,018	D	3
C130	70,307	2S	0
Wide-Body Jets			
B747-400	395,986	2D/2D2	2
B767-300	185,519	2D	14
MD11 Series	281,680	2D	5
DC10-10	219,992	2D	0
DC10-30	264,444	2D/D1	0
A380	591,995	2D/3D2	0
Light Bus Jets	11,340	D	2,223
CIT3/CNA/FAL50/BEC58P			
GASEPF/GASEDV/Lear Jet			
MU3001			
SD330/SF340			
Heavy Bus Jets	34,927	D	5
GIIB/GIV/GV			
CL600/CL601			
Commuters	21,092	D	296
DHC Series			
EMB Series			
Total			2,604

*Note:
– D = Dual Wheel
– 2D = Dual Tandem
– 2S = Two Singles in Tandem

subgrade CBR and modulus were computed for a test section and used for the structural analysis as inputs. Further, the traffic forecast data used for the test section were obtained and used in the structural analysis. The traffic forecast is summarized in Table 3, "Design Traffic.

3. CTE Measurements

To investigate the behavior of a concrete pavement in an airport under both traffic loading and environmental loading on the PCC layer, the CTE of the concrete mixture was measured in the lab for structural analysis. Granite coarse aggregate and alluvial/marine natural fine sand for use in the airport pavement test section were respectively prepared in accordance with grading requirements No. 57 and No. 10 from the ASTM C33 specification, "Standard Specification for Concrete Aggregates." The mix designs that are used in PCC pavement construction were utilized in this study to measure the CTE of an actual PCC mixture. To prepare the specimens used to measure the CTE, granite coarse aggregate and natural sand with 3% or 6% fly ash and a 3% or 6% air-entraining admixture were used in the mix design. Five specimens were prepared from the mixture for the CTE measurement. A total of forty (40) specimens were subjected to the CTE measurements.

Table 4 summarizes the mix designs of the eight different mixtures. To properly account for the effect of aggregate content changes on the CTEs, the slump was held at approximately 50 mm in all the concrete mixture designs, by adjusting the amount of water used in the mixes. Thus, the water cement ratio varied from 0.45 to 0.6. The concrete mixing procedure was in accordance with AASHTO T 126 using a portable drum mixer. While preparing each batch, traditional tests on fresh mixes (ASTM C 231, air content using pressure meter; ASTM C 143, slump test; ASTM C 31, specimen molding; and ASTM C 138, unit weight of fresh mix) were also performed. AASHTO recently adopted AASHTO T 336-11 as the new standard test method. Therefore, AASHTO T 336-11 was used to measure the CTEs of the concrete mixtures in this study. Pine Instrument Company's AFCT2 system was used for determining the CTEs of the concrete samples to meet the requirements of the AASHTO T336-11 protocol. Table 5 shows the results of the CTE measurements. The average CTE of granite concrete with natural sand was 4.906 με/°F (8.831 με/°C), with a standard deviation of 0.177 με/°F (0.319 με/°C).

Table 4. Concrete Mix Design for CTE Test

Mix No.	Granite (kg/m^3)	NS (kg/m^3)	C-Ash (kg/m^3)	F-Ash (kg/m^3)	Cement (kg/m^3)	Air Content
1	1244	563	11.85	0	314	3%
2	1244	563	11.85	0	314	6%
3	1244	563	94.8	0	273	3%
4	1244	563	94.8	0	273	6%
5	1244	563	0	11.85	314	3%
6	1244	563	0	11.85	314	6%
7	1244	563	0	94.8	273	3%
8	1244	563	0	94.8	273	6%

4. Analyses and Results

To analyze the behaviors of airport pavement test sections under temperature-induced loading conditions, a finite element program (EverFE 2.25) was used. The test section of the airport pavement was composed of a concrete slab, Cement-Treated Base (CTB), crushed-stone base, and subbase. As shown in Fig. 2, nine (9) concrete slabs were simulated, where each slab model was created using 20-node solid elements. The joints of the slab and the contacting faces between the pavement layers were modeled by means of 16-node interface elements with no thickness. Dowel bars (D40 × 510 mm) were modeled using

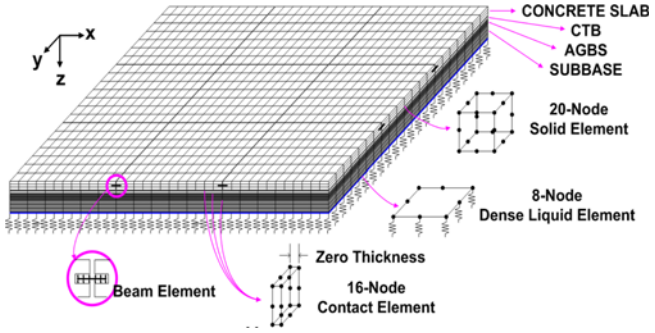

Fig. 2. Finite Element Model

Table 5. Results of CTE Measurements

Mix No.	CTE (/°C)						
	Specimen 1	Specimen 2	Specimen 3	Specimen 4	Specimen 5	Average	Standard Deviation
1	8.7354	9.1350	8.9514	8.874	8.6364	8.8668	0.173
2	9.3672	9.4950	9.1350	9.1548	9.3366	9.2970	0.136
3	8.8632	8.9208	8.8344	8.7948	8.7156	8.8254	0.069
4	9.2268	9.1098	9.0756	9.1494	9.1314	9.1386	0.050
5	8.6238	8.7318	8.6148	8.7192	8.712	8.6796	0.050
6	9.0630	8.9262	8.8794	8.8272	9.009	8.9406	0.085
7	8.5878	8.1936	8.5644	8.2188	8.6832	8.4492	0.203
8	8.2476	8.6058	8.5140	8.7156	8.1540	8.4474	0.213

Table 6. Sizes of Model Components

	Size	Thickness (mm)
Concrete Slab	6 m by 6 m (9 ea)	430
CTB	18 m by 18 m	150
AGBS	18 m by 18 m	300
Subbase	18 m by 18 m	600
Dowel bar	D40 mm by L510 mm	-

Table 7. Material Properties of Model Components

	Elastic Modulus (MPa)	Poisson's ratio	Density (t/m^3)	CTE (/°C)
Concrete Slab	27,600	0.15	2.5	8.831×10^{-6}
CTB	3,448	0.20	2.2	-
AGBS	517	0.30	2.0	-
Subbase	176	0.35	1.9	-
Dowel bar	200,000	0.30	7.0	-
Subgrade	0.03 MPa/mm (bearing capacity factor, K)			

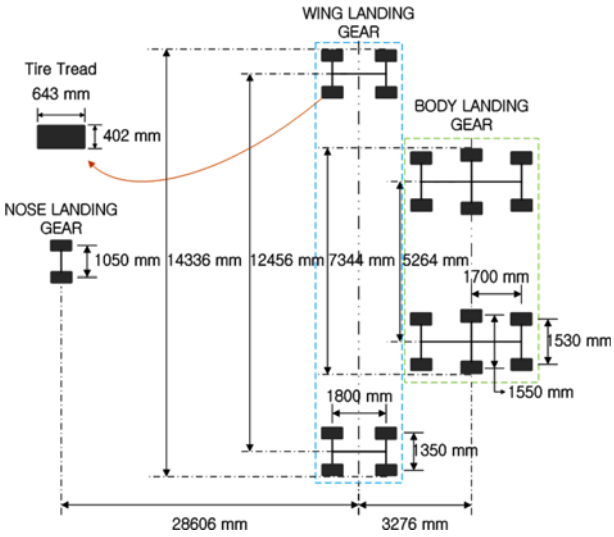

Fig. 3. Landing Gear Footprint of Airbus 380

embedded beam elements with a 460-mm spacing, and were connected to the nodes of the slab by connectors allowing stiffness in only the vertical direction. The subgrade was modeled with 8-node dense liquid elements and tensionless spring elements (Davids, 2003). Table 6 lists the dimensions and thickness of each layer of the airport pavement test section.

The slippage of the slab on the CTB was allowed and modeled, whereas the other layers were tied at the contact faces. The initial slip displacement and friction stiffness of the contact surface between the concrete slab and CTB were assigned values of 0.274 mm and 10.595 kPa/mm, respectively (Lim *et al*., 2010; Wimsatt *et al*., 1986). The material properties of each layer are summarized in Table 7. As discussed earlier, the subgrade reaction was measured in the FWD test, and typical elastic modulus values were selected for the concrete, CTB, AGBS, and subbase layers based on the references (Bowles, 1996; Pimentel *et al*., 2009; Lim, 2011). The measured CTE, in accordance with AASHTO T 336-11, was used for this analysis.

For the traffic factor, an Airbus 380 was selected; this airliner has the largest maximum takeoff weight among the aircraft types shown in Table 3. The data for the landing gear footprint of the aircraft and the tire size are shown in Fig. 3. The maximum takeoff weight of the A380 is 600,000 kg. Because the wing and body landing gears, which are the main landing gears, support 95% of the load, the load was assigned without considering the nose landing gear. The tire size and pressure for the main landing gear were assigned specifications of 1400 × 530R23 42PR and 1.61 MPa, respectively, for the analysis.

The CTE is influenced by the temperature, which induces a differential volume change between the upper part and lower part of the slab. This in turn causes upward and downward curling. This curling is confined by the self-weight, friction force, and the dowel bar connecting the slab to the adjacent slab, which results in internal stresses. The temperature gradients for the concrete slab of 0.33°C/cm were applied as the temperature load causing the upward and downward curling, which was based on previous research (Masad *et al.*, 1996). The self-weight of the concrete pavement was considered. The main landing gears were positioned at the center of the slab and then shifted vertically and horizontally in 400-mm intervals to measure the magnitudes and positions of the maximum tensile stresses. Around the joints, the model was analyzed using 100-mm intervals for the loading position to minimize the outlier. The pavement behaviors under traffic loadings were analyzed by comparing the maximum tensile stresses and their locations in two different cases: 1) with temperature-induced loading and 2) without temperature-induced loading.

When temperature-induced loading was not taken into consideration, as shown in Fig. 4, little stress was observed

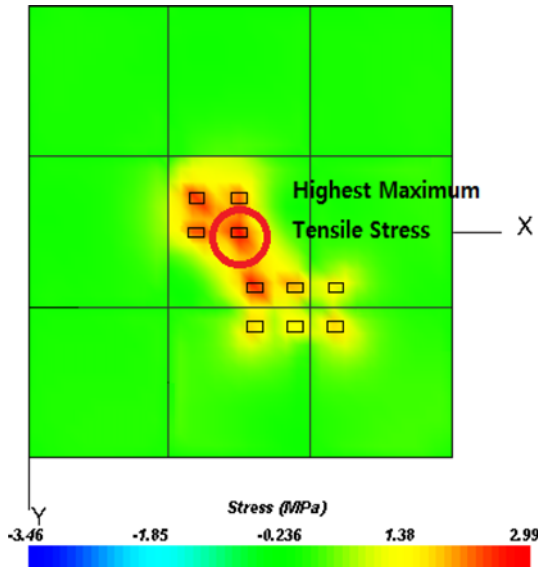

Fig. 4. Stress Distribution at Slab Bottom under Traffic Loading Only

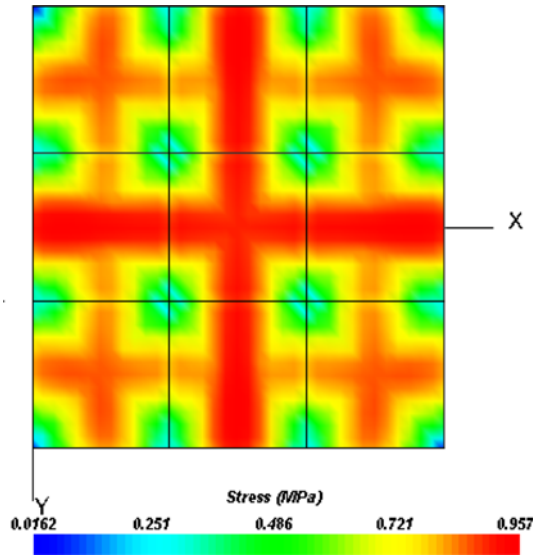

Fig. 5. Stress Distribution at Slab Bottom under Positive Temperature Gradient Only

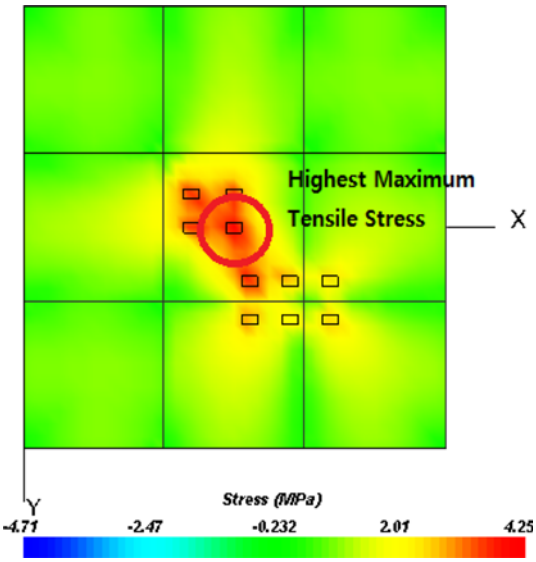

Fig. 6. Stress Distribution at Slab Bottom under Positive Temperature Gradient and Traffic Load

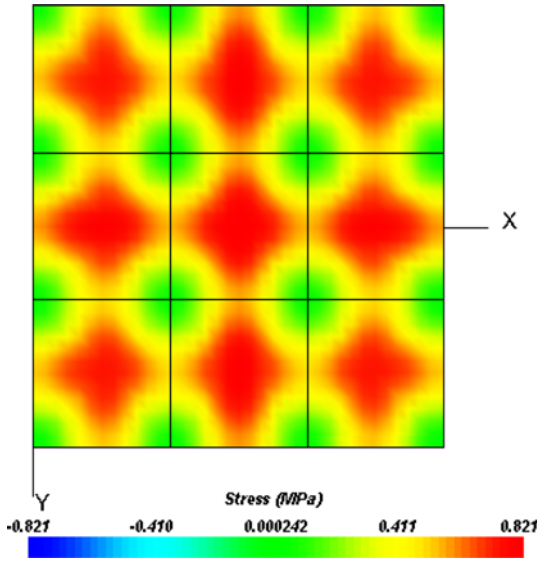

Fig. 7. Stress Distribution at Slab Top under Negative Temperature Gradient Only

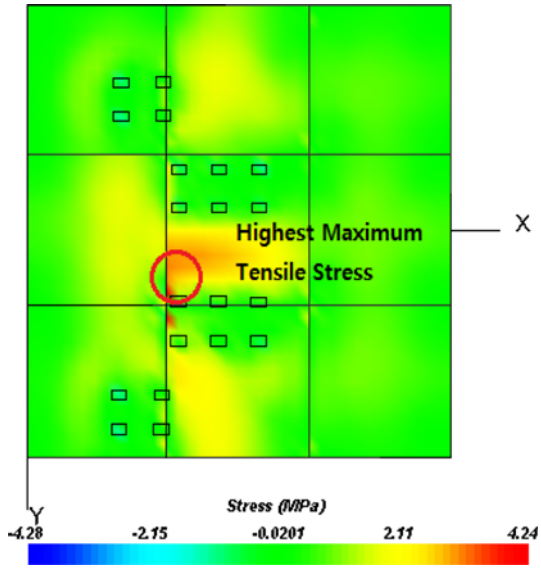

Fig. 8. Stress Distribution at Slab Top under Negative Temperature Gradient and Traffic Load

because there was no volume change in the slab. When a traffic load was applied without a temperature load, a maximum tensile stress of about 3 MPa occurred at the bottom center of the concrete slab. Thus, the distresses at the edge or corner of the slab frequently observed in the field could not be related to the existing design method by only considering the traffic load. Next, the traffic load was applied on the concrete with a positive temperature gradient of +0.33°C/cm, which induced downward curling of the concrete slab. In Fig. 5, it can be seen that tensile stress occurs at the bottom of the slab when temperature-induced loading is applied to the slab. In addition to the temperature loading, the aircraft traffic loading was applied to the concrete slab by shifting the main landing gear from the slab to the adjacent slab. The maximum tensile stresses and the location that provided the largest maximum tensile stress were determined. As a result, as shown in Fig. 6, the gear loading position that induced the largest maximum tensile stress, similar to the case where only traffic loading was applied, was located in the middle of the concrete slab. However, the largest maximum tensile stress was calculated to be 1 MPa higher than in the previous case.

Finally, a concrete slab under traffic loading and a negative temperature gradient was analyzed. A negative temperature gradient of -0.33°C/cm was used as the temperature loading, which induced upward curling. Fig. 7 shows the maximum tensile stress distribution at the center of the top of the slab, caused by upward curling. The main landing gear was applied in the same manner as with the positive temperature gradient, and

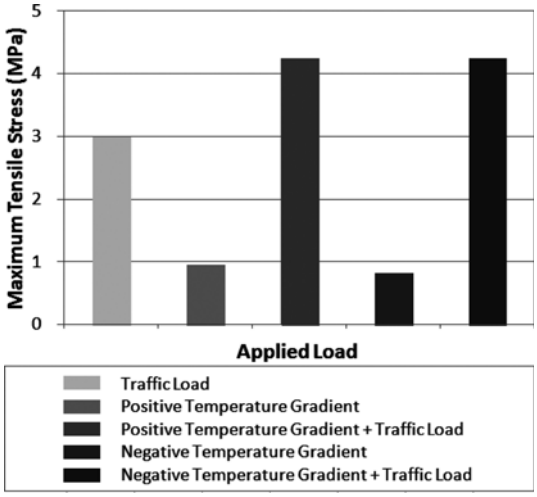

Fig. 9. Highest Maximum Tensile Stress Along with Applied Load

the traffic loading position that induced the largest maximum tensile stress and the position of the maximum tensile stress were calculated, as shown in Fig. 8. The magnitude of the stress was similar to the case of a positive temperature gradient with a traffic load. However, a large tensile stress was observed in the upper corner of the concrete slab with the longitudinal aircraft moving direction. A comparison of the highest maximum tensile stress along with the applied load is shown in Fig. 9. It should be noted that the result tended to correspond with the vulnerable position of the airport pavement slab on which damage occurred frequently.

5. Conclusions

A test section of an airport pavement was analyzed to estimate the tensile stress at the PCC layer using traffic and temperature loading conditions. The FWD test and CTE measurements of PCC were conducted to obtain reasonable input values for structural analyses under various loading conditions. A PCC layer deterioration that was similar to that frequently observed in airport pavement, along with a large tensile stress, was observed in the upper corner of the concrete slab with the longitudinal aircraft moving direction when both the traffic and temperature loadings were taken into consideration. This study substantiated that the CTE of concrete should be taken into consideration in airport pavement design to minimize pavement deterioration. This study suggested the incorporation of the CTE into airport pavement design as an input to improve the performance of airport concrete pavement.

Acknowledgement

This study was sponsored by Inha University research grant and by the research project "Development of Construction and Maintenance Technology for Low-Carbon Green Airport Pavements" funded by the Ministry of Land, Infrastructure and Transport (MOLIT) and the Korea Agency for Infrastructure Technology Advancement (KAIA).

References

American Association of State Highway and Transportation Officials (AASHTO) (2011). "Coefficient of thermal expansion of hydraulic cement concrete." *Standard Specifications for Transportation Materials and Methods of Sampling and Testing*, T 336-11, Washington, D.C., USA.

Bowles, J. E. (1996). *Foundation analysis and design,* 5th Edition, McGraw-Hill Companies, Inc., New York, NY, USA.

Davids, W. G. (2003). *EverFE theory manual*, University of Maine, Orono, Maine, USA.

Federal Aviation Administration (FAA) (2011). *Use of nondestructive testing in the evaluation of airport pavements*, Advisory Circular 150/5370-11A, U.S. Department of Transportation, Washington, D.C., USA.

Kim, S. H. and Jeong, J. H. (2013). "Measurement and prediction of coefficient of thermal expansion of concrete pavement in Georgia." *Proceedings of the 92nd Transportation Research Board Annual Meeting*, TRB, Washington, D.C., USA.

Lim, J. S. (2011). *Experiment and analysis of moisture related aging viscoelastic and thermal expansion characteristic of concrete at early-age*, PhD Thesis, Inha University, Korea.

Lim, J. S., Son, S. C., Liu, J. H., and Jeong, J. H. (2010). "Modeling of friction characteristics between concrete pavement slab and subbase." *Journal of the Korean Society of Road Engineers*, KSRE, Vol. 12, No. 4, pp. 211-218.

Masad, E., Taha, R., and Muhunthan, B. (1996). "Finite-element analysis of temperature effects on plain-jointed concrete pavements." *Journal of Transportation Engineering*, ASCE, Vol. 122, No. 5, pp. 388-398, DOI: 10.1061/(ASCE)0733-947X(1996)122:5(388).

Pimentel, M., Costa, P., Carlos, F., and Figueiras, J. (2009). "Behavior of reinforced concrete box culverts under high embankments." *Journal of Structural Engineering*, ASCE, Vol. 135, Issue 4, pp. 366-375, DOI: 10.1061/(ASCE)0733-9445(2009)135:4(366).

Wimsatt, A. W., McCullough, B. F., and Burns, N. H. (1986). *Methods of analyzing and factors influencing frictional effects of subbases*, Research Report 459-2F, Center of Transportation Research, University of Texas at Austin, Texas, USA.